

Lean NO_x Reduction by Hydrogen over Pt-Supported Rare Earth Oxide Catalysts and Their In Situ DRIFTs Study

Masahiro Itoh,[1] Koji Motoki,[1] Makoto Saito,[1] Jun Iwamoto,[2] and Ken-ichi Machida*[1]

[1]Center for Advanced Science and Innovation, Osaka University, 2-1 Yamadaoka, Suita, Osaka 565-0871

[2]Honda R&D Co., Ltd., Automobile R&D Center, 4630 Shimotakanezawa, Haga-machi, Haga-gun, Tochigi 321-3393

Received December 1, 2008; E-mail: machida@casi.osaka-u.ac.jp

The Pt-supported rare earth oxide (CeO_2, Pr_6O_{11}, Eu_2O_3, and Gd_2O_3) catalysts were prepared and their selective catalytic reduction (SCR) characteristics for NO_x using hydrogen were investigated under 10 vol % excess oxygen conditions. Among them, only the Pt/CeO_2 catalyst provided good NO conversion (ca. 80%) with ca. 40% N_2 selectivity. Other catalysts hardly showed NO_x reduction activity due to the high solid basicity of supporting materials. In situ diffuse reflectance infrared Fourier transform spectroscopy (DRIFTs) measurements for the Pt/CeO_2 catalyst were performed to obtain the specific adsorption bands assigned to NO_3^- species, indicating that NO_x reduction proceeds via formation of such nitrate.

Nitrogen oxides, NO and NO_2 (referred to as NO_x), are mainly emitted from mobile and stationary internal combustion engines. The NO_x discharge has been strictly regulated especially for that emitted from automobiles, since NO_x is one of the leading causes of photochemical smog and acid rain. Selective catalytic reduction (SCR) of NO_x by using NH_3 (including urea systems), CO, hydrocarbon, or H_2 as a reducing agent have been extensively investigated to reduce the NO_x emission from automobiles.[1–8] Among them, H_2-SCR of NO_x on Pt catalysts is a promising candidate under oxygen-rich conditions such as lean fuel/air ratio combustion. H_2-SCR of NO_x has an advantage of high deNO_x at relatively low temperature, which is relevant for diesel applications with low temperature exhaust gas. Additionally, on-board hydrogen generation can be performed by controlling engine emission mode or using reforming and exhaust gas recirculation systems.[9] There is, however, an important drawback of the H_2-SCR of NO_x on Pt catalysts. It tends to produce more N_2O causing greenhouse warming rather than N_2. The N_2 selectivity, N_2 ratio in reduced products, can be improved by changing the acidity/basicity of support oxides rather than Pt loading or H_2 concentration in the feed gas.[10]

In this study, some rare earth oxides were examined as a support material for Pt metal catalyst. It is well known that the atomic radius of lanthanoid elements (La–Lu) shrinks with increasing atomic number due to the insufficient shielding effect of 4f-electrons against nuclear charge (lanthanoid contraction).[11] The smaller the ionic radius of the cation, the higher the solid acidity of the metal oxide, making it possible to control the solid acidity/basicity by using a series of rare earth (lanthanoid) oxides as a support. In the present study, Pt metal catalysts supported on rare earth oxides (CeO_2, Pr_6O_{11}, Eu_2O_3, and Gd_2O_3) were prepared and their H_2-SCR activity of NO_x under oxygen-rich conditions was investigated from the viewpoint of solid acidity/basicity. Furthermore, in situ DRIFTs measurements were performed in order to elucidate the mechanistic differences, which corresponds the different NO_x reduction behavior between Pt/CeO_2 and other catalysts prepared in this study.

Experimental

Pt/REO_x (RE = Ce, Pr, Eu, and Gd) catalysts were prepared by an incipient wetness impregnation method. The rare earth oxides used here were reagent grade produced by Shin-Etsu Chemical Co., Ltd. The quantity of absorbed water of these oxides was measured before the impregnation procedure. Then each metal oxide was added to the corresponding volume of $Pt(NO_3)_2$ aqueous solutions at 1 wt % Pt loading and mixed thoroughly to get slurries. For CeO_2, the Pt loading was varied from 0.2 to 1.0 wt %. The resulting slurries were dried at 120 °C overnight and then calcined at 600 °C for 2 h in air.

Nitrogen adsorption under 0.03 MPa of N_2 was measured at liquid nitrogen temperature to evaluate the specific surface area using a BET equation. The Pt metal size was calculated from H_2-chemisorption measurements as molecular hydrogen is dissociatively chemisorbed on Pt metal (H/Pt = 1).[12] Temperature-programmed desorption of CO_2 (CO_2-TPD) was used to determine the base properties of catalysts. Before starting CO_2-TPD experiments, the sample was heated in He at 600 °C for 1 h to remove any adsorbed impurities, and then CO_2 was adsorbed on the catalysts at room temperature. The spectra were collected by a mass spectrometer (Pfeiffer Vacuum, Prisma QMS200) in a He stream with a temperature ramp of 10 °C min^{-1}. The sample surface area contacting CO_2 roughly set to 1.0 m^2 for all specimens by adjusting their weight. In a similar way, H_2-TPD experiments were also done to evaluate hydrogen adsorption ability. Sample morphology was observed by a transmission electron microscope (JEOL, JEM-2010F).

Catalytic testing was performed at atmospheric pressure in a conventional fixed-bed quartz reactor. Gas mixtures of 0.1 vol % NO, 0.4 vol % H_2, 10 vol % O_2, and balanced with N_2 were fed to the catalyst sample with 0.15 g ($W/F = 0.3$ g s mL^{-1}) placed in the reactor tube. The effluent from the reactor was analyzed by an

Published on the web September 9, 2009; doi:10.1246/bcsj.82.1197

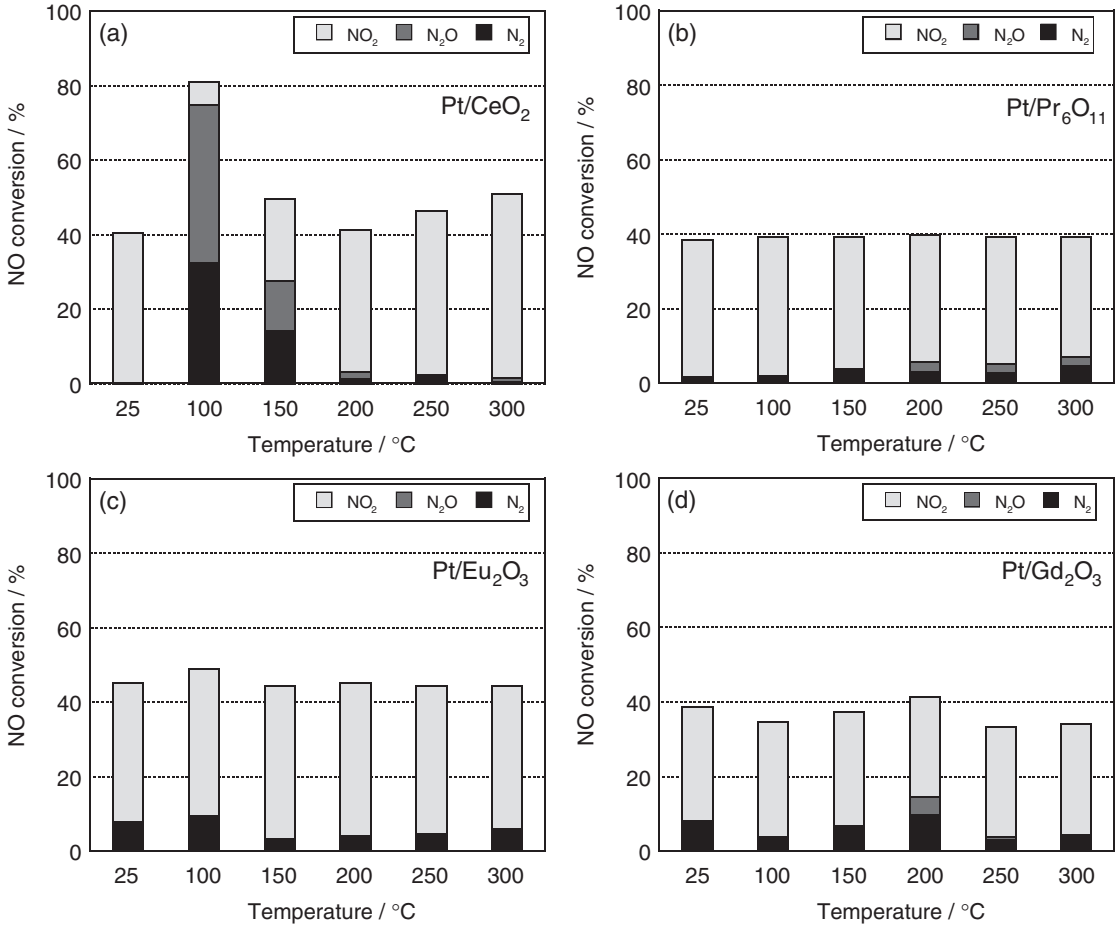

Figure 1. NO_x conversion and product selectivity as a function of temperature observed on (a) Pt/CeO_2, (b) Pt/Pr_6O_{11}, (c) Pt/Eu_2O_3, and (d) Pt/Gd_2O_3 in a stream of 0.1 vol % NO, 0.4 vol % H_2, and 10 vol % O_2. Light gray, dark gray, and black bars represent the NO_2, N_2O, and N_2 selectivity, respectively. The Pt loading is 1.0 wt % for the above catalysts.

online FT-IR spectrometer with a gas cell (Perkin-Elmer, Spectrum 2000). Spectra were collected by scanning 5 times from 1000 to 4000 cm^{-1} at a resolution of 0.5 cm^{-1}. Concentrations of NO, NO_2, N_2O, and NH_3 were calculated from their calibration curves by integrating the peak area at 1911, 1586, 2214, and 1120 cm^{-1}, respectively. The N_2 production was estimated by subtracting NO, NO_2, and N_2O concentrations of outlet gas from the inlet NO concentration. In situ DRIFTs measurements were performed using the above spectrometer with a temperature controllable diffuse reflectance reaction cell. Before the DRIFTs measurements, the samples were treated in a N_2 stream at 450 °C for 1 h to remove adsorbed carbonates.

Results and Discussion

Figure 1 shows the NO conversion with NO_2, N_2O, and N_2 selectivity on the catalysts (Pt: 1.0 wt %) prepared in this study as a function of the reaction temperatures. Pt/CeO_2 showed good NO_x reduction activity with a N_2 selectivity of ca. 40%. No ammonia formation was observed under these reaction conditions. On the other hand, other catalysts provided poor $deNO_x$ activity, similar to the case of using no catalyst. Their BET surface area values are almost same at 8–10 $m^2\,g^{-1}$. The DRIFTs measurements revealed that the difference in $deNO_x$ activity is ascribable to the distinct adsorbed chemical species as shown in Figure 2. All the spectra were referred to a background spectrum in a N_2 flow before introducing NO, O_2, and H_2 gases. It was difficult to assign all the characteristics in the 1000–1650 cm^{-1} region because there were various chemical adsorption species overlapping each other. On the spectrum for Pt/CeO_2 (spectrum a), the absorption bands assigned to NO_3^- appeared at 1316, 1435, 1530, and 1617 cm^{-1}, and the other bands at 1694 and 1766 cm^{-1} were attributed to Pt–NO stretching vibration.[13] Meanwhile, the main absorption band at 1189 cm^{-1} was assigned to chelating nitrite species (NO_2^-) and a weak absorption band corresponding to the nitrate species was observed at 1431 cm^{-1} on the DRIFT spectra for the other catalysts (spectrum b typically observed on Pt/Eu_2O_3).[14] The pattern of spectrum b is quite similar to those observed on sole oxides. It indicates rare earth oxides such as Pr_6O_{11}, Eu_2O_3, and Gd_2O_3 decrease the dissociation ability of Pt metal. In fact, the hydrogen adsorption ability of Pt on Eu_2O_3 is weaker than that on CeO_2, which was checked by H_2-TPD measurements as illustrated in Figure 3. Figure 4 shows the CO_2-TPD profiles for Pt/REO_x catalysts. The CO_2 desorption peaks at around 250–400 °C on the Pt/Pr_6O_{11}, Pt/Eu_2O_3, and Pt/Gd_2O_3 catalysts suggest the presence of solid basicity. On the other hand, the Pt/CeO_2 catalyst gave only a small desorption peak at around 100 °C, indicating weak basicity. This tendency well

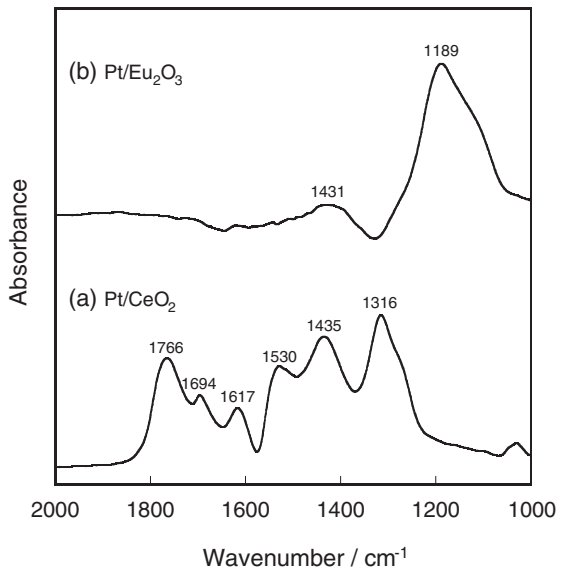

Figure 2. DRIFT spectra obtained at 100 °C in a stream of 0.1 vol % NO, 0.4 vol % H_2, and 10 vol % O_2 on (a) Pt/CeO_2 and (b) Pt/Eu_2O_3. The Pt loading is 1.0 wt %.

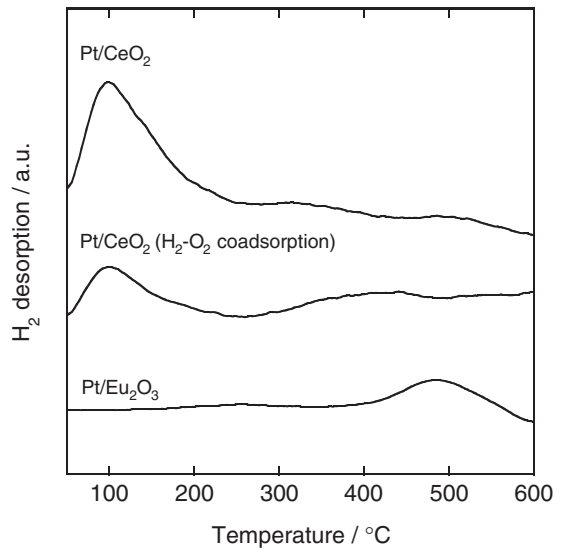

Figure 3. H_2 temperature-programmed desorption profiles on Pt/CeO_2 and Pt/Eu_2O_3, together with H_2 desorption profile after coadsorption of H_2 and O_2 for Pt/CeO_2. The Pt loading is 1.0 wt %.

agrees with results reported by Sato et al.[15] Since a NO_x reduction reaction under excess oxygen can occur on a Pt/MgO catalyst with strong solid basicity,[16] the above deactivation of Pt metal by the Pr_6O_{11}, Eu_2O_3, and Gd_2O_3 supports is probably due to specific interaction between the metal and the support.

Figure 5 shows the dependence of the deNO_x activity on the Pt loading for Pt/CeO_2. The optimal NO_x reduction temperatures were 200, 150, and 100 °C for Pt loading of 0.2, 0.5, and 1.0 wt %, respectively. The respective Pt metal particle sizes are 4, 7, and 12 nm for 0.2, 0.5, and 1.0 wt % loading. The particle size evaluated from the H_2 chemisorption is almost coincident with that directly observed by a TEM measurement as seen in Supporting Information. The optimal temperature for the NO_x

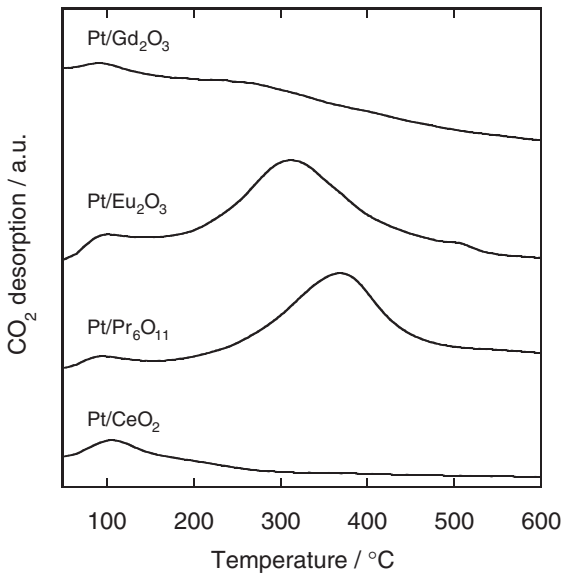

Figure 4. CO_2 temperature-programmed desorption profiles on Pt/CeO_2, Pt/Pr_6O_{11}, Pt/Eu_2O_3, and Pt/Gd_2O_3. The Pt loading is 1.0 wt %.

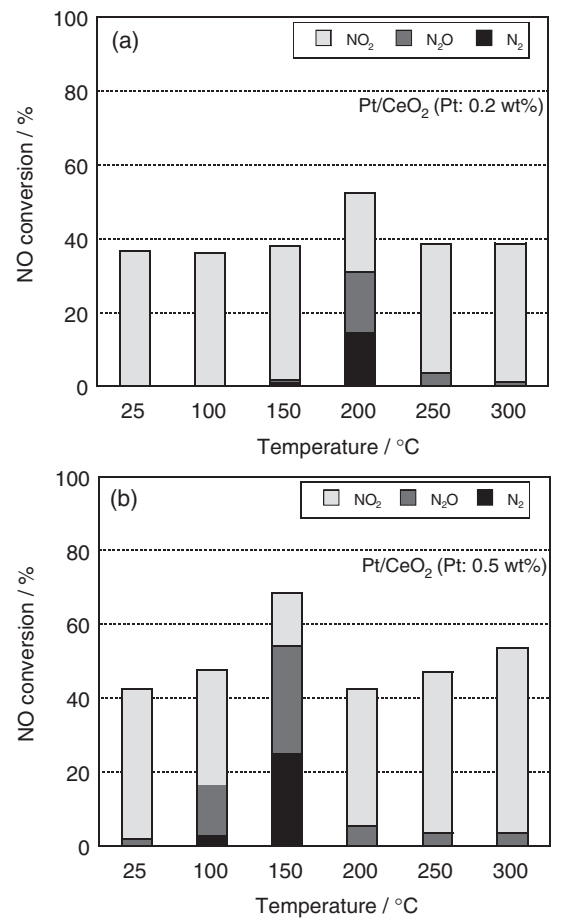

Figure 5. NO_x conversion and product selectivity as a function of temperature observed on Pt/CeO_2 in a stream of 0.1 vol % NO, 0.4 vol % H_2, and 10 vol % O_2 with (a) Pt loading of 0.2 wt % and (b) Pt loading of 0.5 wt %.

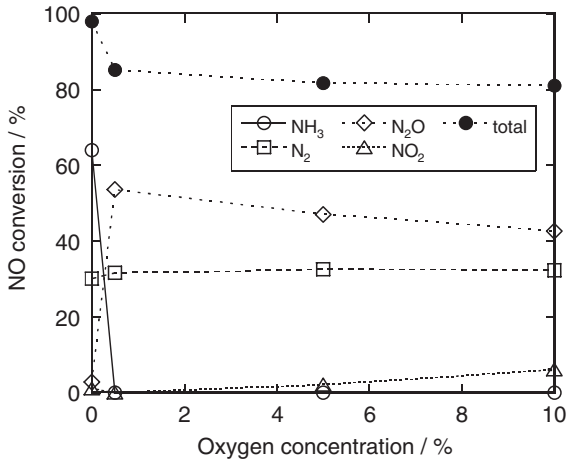

Figure 6. Oxygen concentration dependence on NO_x conversion and product selectivity as a function of temperature observed on Pt/CeO_2 (Pt: 1.0 wt %) in a stream of 0.1 vol % NO, 0.4 vol % H_2, and 0–10 vol % O_2.

reduction increased with decreasing Pt metal size. Similar particle size dependence was observed on Pt/Al_2O_3 catalysts prepared by a solvothermal method, indicating that Pt metal powder with a larger particle size provides higher hydrogenation activity.[17] Although a suitable Pt loading method should be explored to obtain high metal dispersion, this particle size dependence for the deNO_x activity may allows us to regulate the NO_x reduction temperature.

In order to examine the present NO_x reduction mechanism, oxygen concentration dependence of the N_2, NH_3, N_2O, and NO_2 yields was measured at 100 °C on Pt/CeO_2 (Pt: 1.0 wt %) as shown in Figure 6. The total NO conversion sharply declined by addition of a little oxygen gas (0.5 vol %) and then gradually decreased with increasing oxygen concentration. Ammonia was preferentially formed in the absence of oxygen, but the N_2, N_2O, and NO_2 yields were not strongly dependent on the oxygen concentration (0.5–10 vol %). When the oxygen concentration was fixed at 0.5 vol %, increasing hydrogen concentration to 0.8 vol % almost completely recovered the NO conversion to ca. 100%, having respective N_2 and N_2O yields of 170 and 630 ppm, together with a trace of NO_2 (not shown in a figure). Further increasing hydrogen concentration up to 1.6 vol % provided similar NO reduction behavior under anoxic conditions (NO conversion: ca. 100%, N_2 yield: 140 ppm, NH_3 yield: 710 ppm, and a trace of NO_2). A H_2-TPD measurement on Pt/CeO_2 (Pt: 1.0 wt %) after H_2 (0.4 vol %) and O_2 (10 vol %) coadsorption resulted in decreasing H_2 adsorption as shown in Figure 2. These results indicate that oxygen adsorption retards H_2 and NO attacking Pt metal to decrease the NO conversion and to suppress the NH_3 formation.

The reaction scheme between NO and H_2 seems to be different with or without oxygen, as the ammonia formation was strictly suppressed by the existence of oxygen. Figure 7 shows the DRIFT spectra obtained on Pt/CeO_2 (Pt: 1.0 wt %) with or without oxygen. In the absence of oxygen (spectrum a), a specific adsorbed species assigned to dimeric NO ($N_2O_2^-$) was observed at 1368 cm^{-1}.[18] Absorption bands at 1529 and 1587 cm^{-1} arose from nitrate ion species. Other peaks at 1687 and 1736 cm^{-1} were due to Pt–NO stretching as described

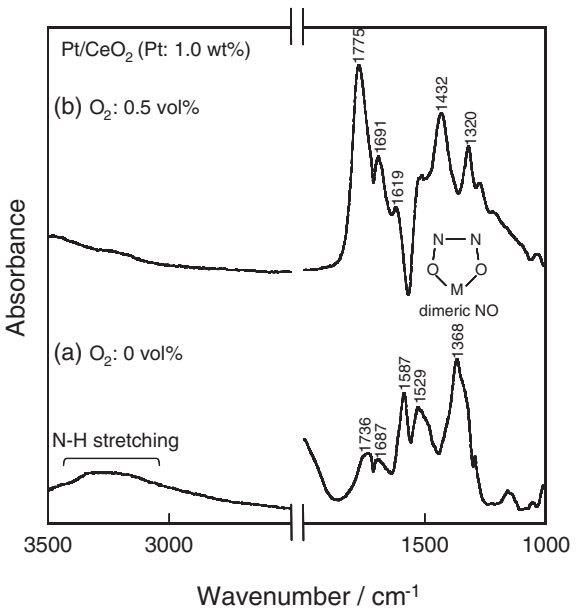

Figure 7. DRIFT spectra obtained on Pt/CeO_2 (Pt: 1.0 wt %) at 100 °C in a stream of 0.1 vol % NO and 0.4 vol % H_2 in (a) the absence of oxygen and (b) 0.5 vol % oxygen.

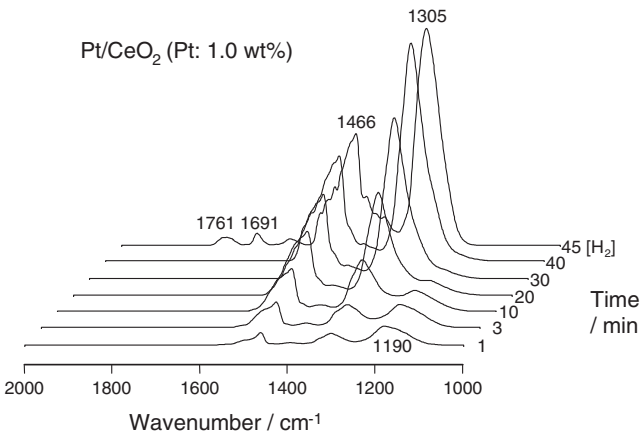

Figure 8. Time-resolved DRIFT spectra obtained on Pt/CeO_2 (Pt: 1.0 wt %) at 100 °C following switch from a stream of N_2 (background gas) to 0.1 vol % NO and 10 vol % O_2. The feed gas composition changed to 0.1 vol % NO, 0.4 vol % H_2, and 10 vol % O_2 at 45 min, represented as 45 [H_2] in the figure.

above. A typical absorption band (1430 cm^{-1}) related to ammonia was not detected,[19] but a weak feature of N–H stretching modes developed in the 3100–3300 cm^{-1} region.[20] In the presence of 0.5 vol % oxygen (spectrum b), adsorbed species were similar to those observed in the presence of 10 vol % oxygen. The DRIFTs measurements imply that ammonia is generated by hydrogen attacking the adsorbed species of dimeric NO and NO was reduced to N_2 through the formation of adsorbed nitrate species regardless of the oxygen concentration. Time-dependent accumulation of nitrate on Pt/CeO_2 (Pt: 1.0 wt %) with flowing gas mixtures of 0.1 vol % NO and 10 vol % O_2 is shown in Figure 8. The DRIFT spectra mainly consisted of adsorbed nitrite (1190 cm^{-1}) and nitrate (1305 and 1466 cm^{-1}) species. Nitrite was the dominant

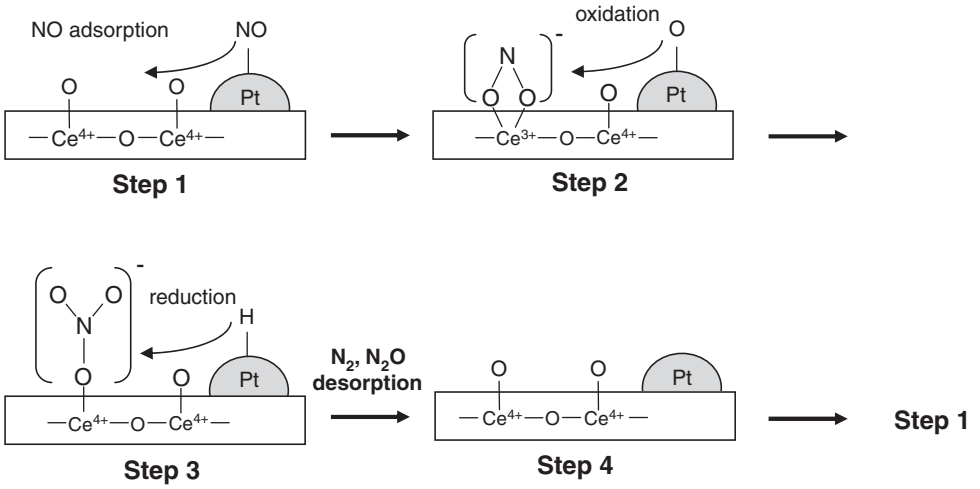

Figure 9. Plausible reaction scheme of NO_x reduction by hydrogen on the present Pt/CeO_2 catalyst.

adsorbed species in the initial state, however the nitrite absorption band decayed with time and finally disappeared after 30 min. On the contrary, nitrate absorption bands continuously increased with time. It indicates that the nitrate species is formed by oxidation of nitrite on the catalyst surface. After 45 min of measurement, 0.4 vol % of hydrogen gas was added to the above feed gas. The new peaks (1691 and 1761 cm^{-1}) assigned to Pt–NO stretching emerged without changing the peak pattern related to the nitrate species, and weak absorption (2200 cm^{-1}) due to gaseous N_2O was observed at the same time. This appearance of Pt–NO stretching bands suggests that the evolution of N_2O by-product came from the reduction of nitrate species. Here, the DRIFT measurement on the sole CeO_2 provided the nitrite absorption band at 1190 cm^{-1} and such nitrite species hardly changed to nitrate after introducing NO and O_2 mixed gases for 30 min. This result suggests that Pt metal is essential for oxidation of the nitrite species and probably for the subsequent reduction of the nitrate species.

Taking the above results into account, a plausible NO_x reduction mechanism on the present Pt/CeO_2 catalyst is shown in Figure 9. First, nitrite species is formed by reacting NO with oxygen in the lattice of CeO_2 and then further oxidation proceeds to generate the nitrate species. The resultant nitrate species are reduced to N_2 or N_2O by hydrogen attacking. An important clue to enhance the N_2 selectivity would be promotion of hydrogenation activity in the nitrate reduction step. Similar oxidation and reduction schemes were proposed by Machida et al. on the MnO_x–CeO_2 and Pt/TiO_2–ZrO_2 systems.[21–23] For the former system, only MnO_x can work as a oxidation site because of the lack of oxidizing ability for CeO_2. In this study, the oxidizing ability of CeO_2 is also poor for conversion of nitrite to nitrate without the Pt metal. The Pt metal plays an important role for the nitrate formation (oxidation) and nitrate reduction (hydrogenation).

Conclusion

The Pt-supported rare earth oxide catalysts were prepared and their NO_x reduction activity was measured in order to investigate the relationship between solid acidity/basicity of the supports and NO_x reduction activity. The acidity/basicity of the supports significantly affects the $deNO_x$ activity and weakly basic metal oxide was found to be suitable as a support for $deNO_x$ Pt catalysts. The results of oxygen concentration dependence on the $deNO_x$ activity indicate that the NO and H_2 adsorption is retarded by oxygen poisoning and such poisoning results in the slight decrease of the NO_x conversion. NH_3 is generated by reacting NO with H_2 via the formation of a dimeric NO adsorbed species in the absence of oxygen, but NH_3 formation is strongly suppressed by adding a little oxygen gas due to poisoning. The NO_x reduction in the presence of oxygen proceeds by hydrogen attacking the adsorbed nitrate species, which is derived from the oxidation of the adsorbed nitrite species.

This work was partly supported by a Grant-in-Aid for Scientific Research on Priority Area A of "Panoscopic Assembling and High Ordered Functions for Rare Earth Materials" from the Ministry of Education, Culture, Sports, Science and Technology.

Supporting Information

Figure S1 is a TEM image of Pt/CeO_2 (Pt: 1.0 wt %). This material is available free of charge on the web at: http://www.csj.jp/journals/bcsj/.

References

1 M. Iwamoto, H. Yahiro, Y. Ta-u, S. Sundo, N. Mizuno, *Shokubai* **1990**, *32*, 430.
2 R. Burch, P. J. Millington, A. P. Walker, *Appl. Catal., B* **1994**, *4*, 65.
3 K. Sakurai, Y. Okamoto, T. Imanaka, S. Teranishi, *Bull. Chem. Soc. Jpn.* **1976**, *49*, 1732.
4 M. Markvart, Vl. Pour, *J. Catal.* **1967**, *7*, 279.
5 M. Koebel, M. Elsener, T. Marti, *Combust. Sci. Tech.* **1996**, *121*, 85.
6 K. Shimizu, A. Satsuma, *Appl. Catal., B* **2007**, *77*, 202.
7 M. Machida, S. Ikeda, *J. Catal.* **2004**, *227*, 53.
8 C. N. Costa, P. G. Savva, J. L. G. Fierro, A. M. Efstathiou, *Appl. Catal., B* **2007**, *75*, 147.

9 A. Abu-Jrai, A. Tsolakis, A. Megaritis, *Int. J. Hydrogen Energy* **2007**, *32*, 3565.
10 M. Machida, T. Watanabe, *Appl. Catal., B* **2004**, *52*, 281.
11 N. E. Topp, *Chemistry of the Rare-Earth Elements*, Elsevier, Amsterdam, **1965**.
12 E. C. Corbos, X. Courtois, F. Can, P. Marécot, D. Duprez, *Appl. Catal., B* **2008**, *84*, 514.
13 N. Macleod, R. M. Lambert, *Appl. Catal., B* **2002**, *35*, 269.
14 C. N. Costa, A. M. Efstathiou, *J. Phys. Chem. C* **2007**, *111*, 3010.
15 S. Sato, R. Takahashi, T. Sodesawa, A. Igarashi, H. Inoue, *Appl. Catal., A* **2007**, *328*, 109.
16 M. Machida, T. Watanabe, S. Ikeda, T. Kijima, *Catal. Commun.* **2002**, *3*, 233.
17 M. Itoh, N. Tajima, J. Iwamoto, K. Machida, in preparation.
18 S. Philipp, A. Drochner, J. Kunert, H. Vogel, J. Theis, E. S. Lox, *Top. Catal.* **2004**, *30–31*, 235.
19 K. Shimizu, J. Shibata, A. Satsuma, *J. Catal.* **2006**, *239*, 402.
20 N. Macleod, R. Cropley, J. M. Keel, R. M. Lambert, *J. Catal.* **2004**, *221*, 20.
21 M. Machida, S. Ikeda, D. Kurogi, T. Kijima, *Appl. Catal., B* **2001**, *35*, 107.
22 M. Machida, M. Uto, D. Kurogi, T. Kijima, *J. Mater. Chem.* **2001**, *11*, 900.
23 M. Machida, M. Uto, D. Kurogi, T. Kijima, *Chem. Mater.* **2000**, *12*, 3158.